Article

Nanoporous Magnets of Chiral and Racemic [{Mn(HL)}Mn{Mo(CN)}] with Switchable Ordering Temperatures (T = 85 K 106 K) Driven by HO Sorption (L = *N*,*N*-Dimethylalaninol)

Julie Milon, Marie-Christine Daniel, Abdellah Kaiba, Philippe Guionneau, Stphane Brands, and Jean-Pascal Sutter

J. Am. Chem. Soc., **2007**, 129 (45), 13872-13878• DOI: 10.1021/ja073612t • Publication Date (Web): 17 October 2007

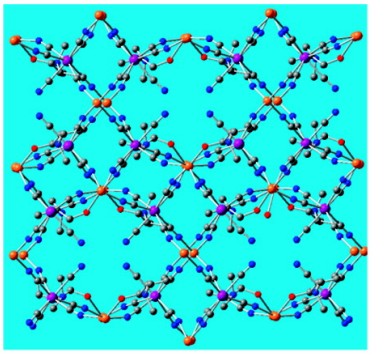

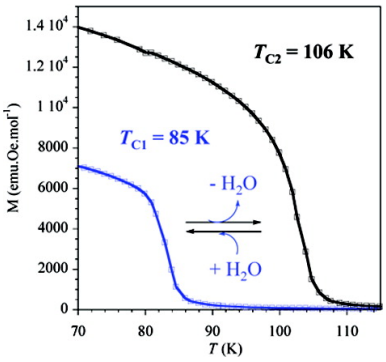

More About This Article

Additional resources and features associated with this article are available within the HTML version:

- Supporting Information
- Links to the 17 articles that cite this article, as of the time of this article download
- Access to high resolution figures
- Links to articles and content related to this article
- Copyright permission to reproduce figures and/or text from this article

View the Full Text HTML

J|A|C|S
ARTICLES
Published on Web 10/17/2007

Nanoporous Magnets of Chiral and Racemic $[\{Mn(HL)\}_2Mn\{Mo(CN)_7\}_2]$ with Switchable Ordering Temperatures (T_C = 85 K ↔ 106 K) Driven by H_2O Sorption (L = *N*,*N*-Dimethylalaninol)

Julie Milon,[†] Marie-Christine Daniel,[‡] Abdellah Kaiba,[‡] Philippe Guionneau,[‡] Stéphane Brandès,[§] and Jean-Pascal Sutter*[,†,‡]

Contribution from the Laboratoire de Chimie de Coordination du CNRS, Université Paul Sabatier, 205, Route de Narbonne, F-31077 Toulouse, France, Institut de Chimie de la Matière Condensée de Bordeaux − ICMCB-CNRS, Université Bordeaux 1, 87 Avenue du Dr. Schweitzer, F-33608 Pessac, France, and ICMUB-UMR 5260, Université de Bourgogne, 9 avenue Alain Savary, BP 47870, 21078 Dijon Cedex, France

Received May 20, 2007; E-mail: sutter@lcc-toulouse.fr

Abstract: Molecule-based solids represent a rare opportunity to combine, adjust, and interrelate structural and physical functionalities to develop multifunctional materials. Here we report on a series of porous supramolecular magnets whose magnetic properties are related to their sorption state. A family of magnets of the formula $[\{Mn(HL)(H_2O)\}_2Mn\{Mo(CN)_7\}_2]\cdot 2H_2O$ have been obtained by assembling the heptacyanometalate building unit $\{Mo(CN)_7\}^{4-}$ with Mn(II) in the presence of protonated *N*,*N*-dimethylalaninol (**L**) as ligand, the latter being either as a racemic mixture or as a chiral *R*- or *S*-enantiomer. The resulting magnets possess an open framework structure and exhibit a T_C with a switching behavior (T_C = 85 K ↔ 106 K) as a function of the hydration state. Moreover, chiral magnets are formed with the optically active ligands. The H_2O and gas (N_2, CO_2, CO) sorption features, the magnetic behavior of both the hydrated and dehydrated magnets, and the crystal structures of the hydrated chiral (*S*) and racemic magnets are described.

Introduction

Materials possessing a reversible switch of physical properties in the solid state are of major interest from both an applied and a fundamental point of view. In this respect, magnetic molecular systems have proven to show exceptional versatility. For instance, bistable molecules that exist in two different spin states as a result of a spin crossover behavior or valence tautomerism can be switched from one state to another by an external stimulus such as temperature, pressure, light, or a magnetic field.[1−5] For exchange coupled systems, magnetic ordering triggered by light was observed for Prussian Blue type compounds generating either light-induced magnets or high-spin clusters.[6−9] Likewise the magnetic features could be modulated electrochemically[10] or by pressure.[11−13] In all these cases, it is an energy input that causes either the intra- or the intersite electron transfer which leads to the new state. Another possibility to induce a change of the physical property of a solid would be to modify the ligand (i.e., crystal) field characteristics which in turn could shift the equilibrium between two electronic states[14] or modify the strength of the exchange interactions and hence offers an alternative possibility for property switching. For instance, an alteration in the coordination sphere of one metal site in the solid state for a magnet was shown to induce a shift of T_C from 75 to 106 K.[15] Similarly, the degree of solvation was also found to have a direct consequence on the magnetic feature of magnets.[16−23] In some cases, the process was found

[†] Université Paul Sabatier.
[‡] Université Bordeaux 1.
[§] Université de Bourgogne.

(1) Kahn, O.; Kröber, J.; Jay, C. *Adv. Mater.* **1992**, *4*, 718−728.
(2) Ksenofontov, V.; Gaspar, A. B.; Gütlich, P. In *Spin crossover in transition metal compounds III*; Springer: Berlin, 2004; Vol. 235, pp 23−64.
(3) Bousseksou, A.; Boukheddade, K.; Goiran, M.; Tuchagues, J. P.; Varret, F. *Top. Curr. Chem.* **2004**, *235*, 65−84.
(4) Evangelio, E.; Ruiz-Molina, D. *Eur. J. Inorg. Chem* **2005**, 2957−2971.
(5) Bonhommeau, S.; Molnar, G.; Galet, A.; Zwick, A.; Real, J. A.; McGarvey, J. J.; Bousseksou, A. *Angew. Chem., Int. Ed.* **2005**, *44*, 4069−4073.
(6) Sato, O.; Iyoda, T.; Fujishima, A.; Hashimoto, K. *Science* **1996**, *272*, 704−705.
(7) Escax, V.; Bleuzen, A.; Cartier dit Moulin, C.; Villain, F.; Goujon, A.; Varret, F.; Verdaguer, M. *J. Am. Chem. Soc.* **2001**, *123*, 12536−12543.
(8) Herrera, J. M.; Marvaud, V.; Verdaguer, M.; Marrot, J.; Kaliesz, M.; Mathonière, C. *Angew. Chem., Int. Ed.* **2004**, *43*, 5468−5471.
(9) Ohkoshi, S.; Tokoro, H.; Hozumi, T.; Zhang, Y.; Hashimoto, K.; Mathonière, C.; Bord, I.; Rombaut, G.; Verelst, M.; Cartier, dit Moulin, C.; Villain, F. *J. Am. Chem. Soc.* **2006**, *128*, 270−277.
(10) Sato, O.; Iyoda, T.; Fujishima, A.; Hashimoto, K. *Science* **1996**, *271*, 49−51.
(11) Maeda, T.; Mito, M.; Deguchi, H.; Takagi, S.; Kaneko, W.; Ohba, M.; Okawa, H. *Polyhedron* **2005**, *24*, 2497−2500.
(12) Coronado, E.; Giménez-Lopez, M. C.; Levchenko, G.; Romero, F. M.; Gracia-Baonza, V.; Milner, A.; Paz-Psaternak, M. *J. Am. Chem. Soc.* **2005**, *127*, 4580−4581.
(13) Egan, L.; Kamenev, K.; Papanikolaou, D.; Takabayashi, Y.; Margadonna, S. *J. Am. Chem. Soc.* **2006**, *128*, 6034−6035.
(14) Halder, G. J.; Kepert, C. J.; Moubaraki, B.; Murray, K. S.; Cashion, J. D. *Science* **2002**, *298*, 1762−1765.
(15) Tanase, S.; Tuna, F.; Guionneau, P.; Maris, T.; Rombaut, G.; Mathonière, C.; Andruh, M.; Kahn, O.; Sutter, J.-P. *Inorg. Chem.* **2003**, *42*, 1625−1631.
(16) Kahn, O.; Larionova, J.; Yakhmi, J. V. *Chem.—Eur. J.* **1999**, *5*, 3443−3449.

10.1021/ja073612t CCC: $37.00

to be reversible, but the magnetic characteristics were a function of the actual solvent content of the framework; i.e., the magnets' T_C is modulated by the solvent content rather than switched between two fixed temperatures. We report here that a modification of the magnetic features through solvate sorption is greatly improved if the magnet exhibits an open framework. Supramolecular porous magnets are currently attracting interest because such materials are envisaged as sensors.[24−30] We show that the synergy between sorption and magnetic properties might also generate unprecedented magnets with switchable T_C.

We describe here a family of magnets of the formula $[\{Mn(HL)(H_2O)\}_2Mn\{Mo(CN)_7\}_2]\cdot 2H_2O$ obtained by assembling the heptacyano-metalate unit $\{Mo(CN)_7\}^{4-}$ with Mn(II) in the presence of *N*,*N*-dimethylalaninol (**L**) as ligand; the latter is present either as a racemic mixture or as an optically pure *R*- or *S*-enantiomer. The resulting magnets possess an open framework structure and exhibit a T_C with a switching behavior as a function of the hydration state. Moreover, chiral magnets were obtained with the optically active ligands. The H_2O sorption features and the magnetic behavior of both the hydrated and dehydrated magnets have been investigated, and the crystal structures for the hydrated chiral (*S*) and racemic magnets have been solved.

Results and Discussion

Syntheses and Crystal Structures. $[\{Mn(HL)(H_2O)\}_2Mn\{Mo(CN)_7\}_2]\cdot 2H_2O$, **1**, is obtained either as a microcrystalline powder or as larger crystals by a reaction performed with $K_4\{Mo(CN)_7\}$, $MnCl_2$, and *N*,*N*-dimethylalaninol (**L**) in H_2O. Initial preparations revealed that during this reaction the ligand becomes protonated and traces of pyrochroite, $\{Mn(OH)_2\}$, are formed as a byproduct. This byproduct is not found if the assembly is performed in an acidic solution or with the protonated ligand, i.e., $H\mathbf{L}^+$. Dark green needle-shaped single crystals suitable for X-ray analyses were obtained by slow interdiffusion of an acidified aqueous solution containing the cyano-metalate and **L** and a solution of Mn(II) in H_2O. The preparation of $[\{Mn(HL)(H_2O)\}_2Mn\{Mo(CN)_7\}_2]\cdot 2H_2O$ **1** in larger amounts as a dark green microcrystalline powder is carried out by reacting $\{Mo(CN)_7\}^{4-}$, HL^+, and Mn(II) in neutral H_2O solution. The experimental X-ray powder pattern for a sample prepared following this procedure confirms the selectivity of the assembling process (Figure SI1, Supporting Information). The same procedures apply whether **L** is the *rac*-, *R*-, or *S*-form leading to **1*rac***, **1*R***, and **1*S***, respectively.

Table 1. X-ray Diffraction Experimental and Crystal Data for Compound **1*S*** and **1*rac***

	$[\{Mn(HL)(H_2O)\}_2Mn\{Mo(CN)_7\}_2]\cdot 2H_2O$, **1*S***	$[\{Mn(HL)(H_2O)\}_2Mn\{Mo(CN)_7\}_2]\cdot 2H_2O$, **1*rac***
formula	$C_{24}H_{36}Mn_3Mo_2N_{16}O_6$	$C_{24}H_{36}Mn_3Mo_2N_{16}O_6$
fw	1001.3	1001.3
cryst syst	monoclinic	monoclinic
space group	*C*2	*C*2/*c*
a (Å)	26.085(5)	26.035(5)
b (Å)	13.160(2)	13.180(5)
c (Å)	12.889(2)	12.910(5)
β (deg)	116.32(1)	116.60(1)
V (Å^3)	3966(2)	3961(2)
Z-space group	4	8
Z-formula	4	4
ρ_{calcd} (g·cm^{-3})	1.677	1.679
μ (mm^{-1})	1.60	1.60
collctd reflns	11 968	14 651
indep reflns	7425	4015
R_{int}	0.025	0.032
refined params	460	237
refinement against	F^2	F^2
R	0.029	0.037
$R_{w2}(F^2)$	0.034	0.044

The single-crystal X-ray structure determination was performed for $[\{Mn(HL)(H_2O)\}_2Mn\{Mo(CN)_7\}_2]\cdot 2H_2O$ **1rac** (L = (*rac*)-*N*,*N*-dimethylalaninol) and **1*S*** (L = (*S*)-*N*,*N*-dimethylalaninol), crystal data are given in Table 1. Their supramolecular organizations are essentially equivalent even if they crystallize in different space groups (*C*2/*c* and *C*2). The only difference is found for the *N*,*N*-dimethylalaninol ligand, which occurs in a single enantiomeric form in **1*S*** whereas both of the enantioners are present in **1rac**. In the following section, we will briefly describe the structural features for **1*S***; details for **1rac** can be found in Supporting Information.

$[\{Mn(HL)(H_2O)\}_2Mn\{Mo(CN)_7\}_2]\cdot 2H_2O$, **1*S***, can be described as a 3D polymeric assemblage based on $\{Mo(CN)_7\}$ units and Mn ions. The *N*,*N*-dimethylalaninol unit is protonated at the amine function and is coordinated to the Mn sites through its alcohol O-atom. The cyano-bridged bimetallic network exhibits an open structure with solvate H_2O molecules located in the channels (Figure 1).

The extended structure contains a unique Mo site along with two Mn sites, denoted MnA and MnB as shown in Figure 1. The Mo(III) ion is surrounded by seven CN ligands, one being terminal whereas the six others act as bridges between Mo and Mn ions. Two of these Mo−CN → Mn linkages involve MnA sites, and the remaining four bridge MnB sites. The shape of the $\{Mo(CN)_7\}$ units is best described as a slightly distorted capped octahedron as revealed by Continuous Shape Measures (CShM)[31,32] analysis carried out with SHAPE.[33] The results of this analysis is tabulated in Table SI1 (Supporting Information).

(17) Mathonière, C.; Sutter, J.-P.; Yakhmi, J. V. In *Magnetism: molecules to materials*; Miller, J. S., Drillon, M., Eds.; Wiley-VCH: Weinheim, 2002; Vol. 4, pp 1−40.
(18) Larionova, J.; Kahn, O.; Golhen, S.; Ouahab, L.; Clérac, R. *J. Am. Chem. Soc.* **1999**, *121*, 3349−3356.
(19) Ohkoshi, S.; Arai, K.; Sato, Y.; Hashimoto, K. *Nat. Mater.* **2004**, *3*, 857−861.
(20) Nelson, K. J.; Giles, I. D.; Troff, S. A.; Arif, A. M.; Miller, J. S. *Inorg. Chem.* **2006**, *45*, 8922−8929.
(21) Lu, Z.; Wang, X.; Liu, Z.; Liao, F.; Gao, S.; Xiong, R.; Ma, H.; Zhang, D.; Zhu, D. *Inorg. Chem.* **2006**, *45*, 999−1004.
(22) Martinez-Garcia, R.; Knobel, M.; Reguera, E. *J. Phys. Chem. B* **2006**, *110*, 7296−7303.
(23) Xiang, S.; Wu, X.; Zhang, J.; Fu, R.; Hu, S.; Zhang, X. *J. Am. Chem. Soc.* **2005**, *127*, 16352−16353.
(24) Beauvais, L. G.; Long, J. R. *J. Am. Chem. Soc.* **2002**, *124*, 12096−12097.
(25) Guillou, N.; Livage, C.; Drillon, M.; Férey, G. *Angew. Chem., Int. Ed.* **2003**, *42*, 5314−5317.
(26) Wang, Z.; Zhang, B.; Fujiwara, H.; Kobayashi, H.; Kurmoo, M. *Chem. Commun.* **2004**, 416−417.
(27) Maspoch, D.; Ruiz-Molina, D.; Veciana, J. In *Magnetism: molecules to materials*; Miller, J. S., Drillon, M., Eds.; Wiley-VCH: Weinheim, 2005; Vol. 5.
(28) Maspoch, D.; Ruiz-Molina, D.; Wurst, K.; Domingo, N.; Cavallini, M.; Biscarini, F.; Tejada, J.; Rovira, C.; Veciana, J. *Nat. Mater.* **2003**, *2*, 190−195.
(29) Ohkoshi, S.; Tsunobuchi, Y.; Takahashi, H.; Hozumi, T.; Shiro, M.; Hashimoto, K. *J. Am. Chem. Soc.* **2007**, *129*, 3084−3085.
(30) Wang, Z.; Zhang, Y.; Liu, T.; Kurmoo, M.; Gao, S. *Adv. Funct. Mater* **2007**.
(31) Alvarez, S.; Alemany, P.; Casanova, D.; Cirera, J.; Llunell, M.; Avnir, D. *Coord. Chem. Rev.* **2005**, *249*, 1693−1708.
(32) Casanova, D.; Alemany, P.; Bofill, J. M.; Alvarez, S. *Chem.−Eur. J.* **2003**, *9*, 1281−1295.
(33) Llunell, M.; Casanova, D.; Cirera, J.; Bofill, J. M.; Alemany, P.; Alvarez, S.; Pinsky, M.; Avnir, D. SHAPE, 1.1b ed.; University of Barcelona: Barcelona, 2005.

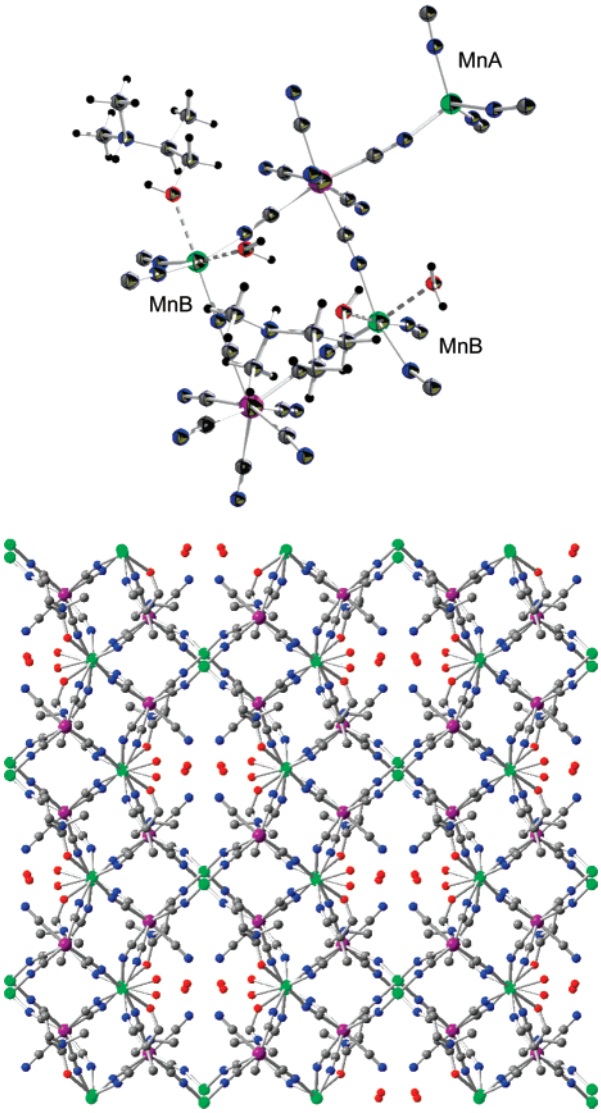

Figure 1. [{Mn(HL)(H$_2$O)}$_2$Mn{Mo(CN)$_7$}$_2$]·2H$_2$O, **1*S***: (*top*) primary assembling pattern; (*bottom*) view of the 3D network along *c*-axis (Mo in purple, Mn in green).

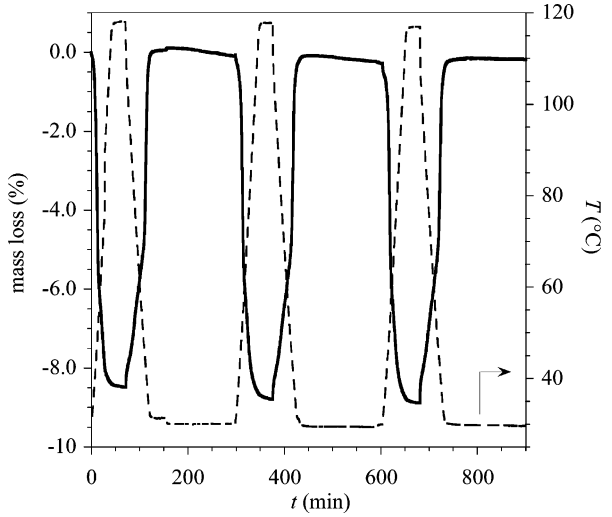

Figure 2. Thermogravimetric analysis for compound **1*S***. The series of heating−cooling cycles reveals a fully reversible sorption process in air as a function of temperature.

The Mo−CN angles are close to linearity spanning from 174.6° to 179.3°. The MnA site has a distorted tetrahedral environment consisting of four NC−Mo linkages, and MnB exhibits a distorted octahedral coordination sphere with four NC−Mo linkages and two O-atoms, one of them corresponding to the alcohol group of *N*,*N*-dimethylalaninol and the second to the oxygen of a H$_2$O ligand. The Mn ← NC bond lengths of the octahedral MnB site range from 2.10(2) to 2.14(1) Å, whereas those of the tetrahedral MnA site are shorter spanning from 2.03-(1) to 2.08(1) Å in agreement with distances found in related organizations.[15] The Mn ← NC angles are found between 163.9° and 178.1° for MnA and between 161.4° and 175.7° for the MnB site. Four H$_2$O molecules per formula unit have been located; two of them act as ligand for the MnB sites, and two are found in the crystal lattice.

Hence, the assemblage of {Mo(CN)$_7$}$^{4-}$ and Mn^{2+} in the presence of ligand **L** generates a 3D cyano-bridged Mn−Mo network where each Mo is linked to six Mn ions and each Mn is linked to four Mo units. Ring shaped channels are formed by four {Mo(CN)$_7$} and four Mn units. Each Mo is linked to two MnA and two MnB sites belonging to two adjacent rings whereas two other CN are coordinated to two Mn ions (MnB) belonging to a neighboring channel. The seventh cyanide is not involved in bridging and points into the channel cavity. The channels are further interconnected by means of the tetrahedral Mn sites that are shared by two channels. It can be noticed that all the metal units are located at the surface of the walls framing the pores. This overall network is reminiscent of a compound reported by Larionova and Clérac.[34] The framework encloses a void in the form of channels running through the structure in which the solvent molecules are located. The volume accessible by a small molecule (H$_2$O) determined with PLATON[35] is 365 Å^3 per unit cell volume (3966 Å^3) which represent 9.2% of potential void per unit volume.

This overall organization is independent of the ligand involved (*rac*-, *R*-, or *S*) during preparation. In the following sections, we will describe the studies carried out on the compounds **1*S*** and **2*S*** (the dehydrated magnet) as representatives, their behaviors, and features apply to all three isomers (i.e., *rac*-, *R*-, or *S*).

Sorption Properties and Framework Stability: The framework of [{Mn(HL)(H$_2$O)}$_2$Mn{Mo(CN)$_7$}$_2$]·2H$_2$O, **1*S*** exhibits channels suggesting an open structure. The capability of this compound to release and take back the solvent molecules it contains has been investigated by thermogravimetric analysis (TGA) and XRPD studies at different temperatures. The TGA depicted in Figure 2 shows a weight loss of 8.5% (4.7 H$_2$O) upon heating to 120 °C corresponding to the release of all the lattice and coordinated H$_2$O. The sorption process is fully reversible, and the system recovers all of its H$_2$O when it stays in air at 298 K. In our experimental conditions, 50 min after heating was stopped, the sorption process had reached completion (Figure 2). The reversibility of the process is confirmed by the XRPD data obtained for a sample at 383 K and after resorption at 298 K; these are compared to the initial sample in Figure 3. These diffractograms reveal a structural phase transition between the hydrated (**1*S***) and dehydrated (**2*S***) forms. This

(34) Larionova, J.; Clérac, R.; Donnadieu, B.; Guérin, C. *Chem.—Eur. J.* **2002**, *8*, 2712−2716.
(35) Spek, A. L. *PLATON, A Multipurpose Crystallographic Tool*; Utrech University: Utrecht, The Netherlands, 2001.

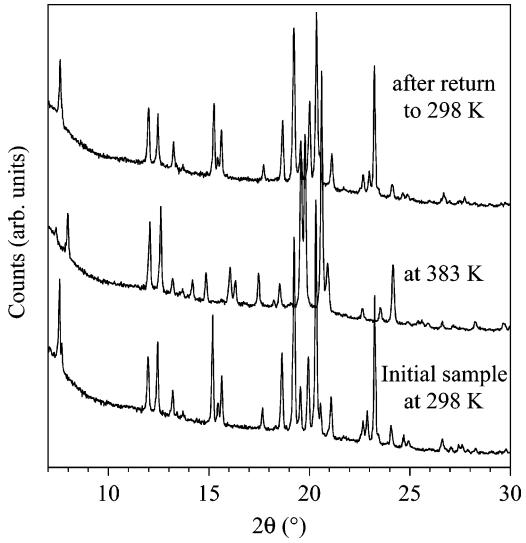

Figure 3. X-ray powder diffractograms recorded for compound **1*S***. (*From bottom to top*) As synthesized at 25 °C, at 110 °C after H_2O release, after return to 25 °C and H_2O readsorption (only the domain $7° < 2\theta < 30°$ is shown).

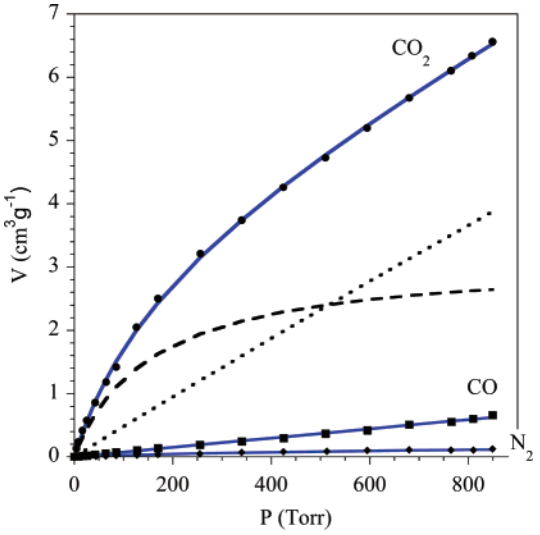

Figure 4. Experimental adsorption isotherms of (●) CO_2, (■) CO, and (◆) N_2 for **2*S*** recorded at 293 K. Calculated isotherms are represented as a thick line. The dashed and dotted curves represent the first and the second components, respectively, of the calculated isotherm for CO_2 adsorption.

transition appears completely reversible after the recovery of the initial phase upon H_2O uptake. Such a behavior points to a certain degree of flexibility of the framework upon guest release and sorption.[36] It can be noticed that the crystallinity of the sample remains unaffected during the sorption process. Nevertheless attempts made with larger crystals revealed that these do not stay single when guest molecules are released.

The removal of H_2O also has an effect on the infrared spectrum. Besides the strong decrease of the absorption band at 3300 cm^{-1}, the CN absorption evolves from a single band (ν = 2092 cm^{-1}) in the hydrated compound **1*S*** to two bands (ν = 2092 and 2022 cm^{-1}) for the dehydrated compound **2*S*** (Figure SI3, Supporting Information).

All these features confirm that $[\{Mn(HL)(H_2O)\}_2Mn\{Mo(CN)_7\}_2]\cdot 2H_2O$, **1*S*** has an open structure capable of efficient, fast, and reversible guest (H_2O) sorption. During the exchange process the integrity of the framework is not affected, and more importantly it is exactly the same phase that is recovered after a desorption−adsorption cycle.

Attempts to measure a BET surface area reveals that the desolvated materials adsorb low amounts of N_2 at 77 K. The adsorption isotherm shows a type II isotherm, and fitting the BET equation to the isotherms gave estimated surface areas of about 15 $m^2\ g^{-1}$. This suggests that the 3D-dimensional framework is less likely to exhibit sustainable porosity upon desolvation, presumably due to the flexibility of the framework which contracts upon H_2O release and hence reduces the potential pores. The apparent contradiction with the efficient adsorption obtained with H_2O might be ascribed to the absence of affinity between N_2 at 77 K and the framework.[36,37]

The gas sorption characteristics of the anhydrous solid **2*S*** were also probed by room temperature isotherm measurements for N_2, CO, and CO_2. As shown in Figure 4, the CO_2 adsorption isotherm at 295 K reveals uptake of 0.27 mmol g^{-1} (6.10 $cm^3\ g^{-1}$) at 760 Torr, which corresponds to 0.26 mol per molecular unit or 0.13 CO_2 adsorbed per molybdenum atom. The experimental CO_2 adsorption isotherms were fitted to a multiple-site adsorption process involving a two Langmuir-type adsorption model,[38,39] and the calculated isotherm is given in Figure 4. Such a model is often required to describe a chemical adsorption process on a surface with heterogeneous energetic interactions. Hence, the CO_2 isotherm recorded at room temperature indicates the presence of two different adsorption sites inside the channels. The first Langmuir-type isotherm describes the adsorption of CO_2 with higher energetic interaction while the second one discloses a very low energetic nonselective adsorption process. The equilibrium constant related to the CO_2 binding affinity, K_i, and the adsorption capacity, V_i, were thus calculated with the adsorption model (see Experimental Section). The experiments evidenced that **2*S*** adsorbs more CO_2 than N_2 and CO. The first process is the main adsorption contribution of the isotherm under low pressure (<200 Torr), and the calculated capacity (V_1 = 3.2 $cm^3\ g^{-1}$) is hardly reached at 760 Torr. Also the main contribution in the higher-pressure range is attributable to the physisorption process. Moreover, the half saturation pressure ($(P_{1/2})_1 = 1/K_1$) for the first process is equal to 160 Torr. This points out the low affinity of the material for CO_2. The CO_2 adsorption greatly contrasts that of other gases owing to its significant quadrupole moment that induces specific interactions with the solid sorbent. However, if we consider the very low specific surface area of the dehydrated solid, almost no adsorption should occur, as in the case of N_2 and CO. But the observed CO_2 adsorption seems to reflect the flexibility of the framework during the adsorption process, as already seen during the hydration/dehydration step.

Previously, 3D microporous metal organic frameworks[40,41] have been shown to exhibit such a breathing phenomenon upon hydration[42,43] or dynamic inclusion of guest[44] which involves structural motion. Hence, pressure-dependent gas adsorption was

(36) Imaz, I.; Bravic, G.; Sutter, J.-P. *Dalton Trans.* **2005**, 2681−2687.
(37) Dybtsev, D. N.; Chun, H.; Yoon, S. H.; Kim, D.; Kim, K. *J. Am. Chem. Soc.* **2004**, *126*, 32−33.
(38) Drago, R. S.; Webster, C. E.; McGilvray, J. M. *J. Am. Chem. Soc.* **1998**, *120*, 538−547.
(39) Brandès, S.; David, G.; Suspène, C.; Corriu, R. J. P.; Guilard, R. *Chem.—Eur. J.* **2007**, *13*, 3480−3490.

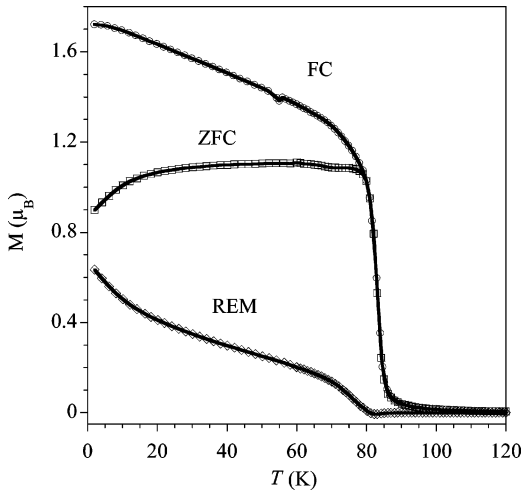

Figure 5. Field cooled magnetization (○, $H = 100$ Oe), zero field cooled (□), and remnant magnetization (◇) as a function of temperature for [{Mn(HL)(H_2O)}$_2$Mn{Mo(CN)$_7$}$_2$]·2H_2O, **1*S***.

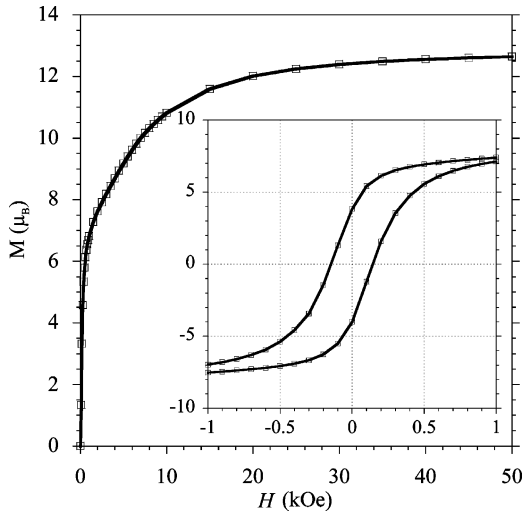

Figure 6. Field dependence of the magnetization and hysteresis loop (*insert*) recorded at 2 K for [{Mn(HL)(H_2O)}$_2$Mn{Mo(CN)$_7$}$_2$]·2H_2O, **1*S***.

observed previously in several flexible porous metal-organic frameworks that exhibit "breathing" or "swelling" effects[44,45] during CO_2, N_2, O_2, or CH_4 adsorption.[46−49] A two-step adsorption process due to opening of the pore when the pressure increases is thus observed. However, the dehydrated form **2*S*** does not show a marked two-step CO_2 adsorption process in the pressure range used which is interpreted as an initial closing of the structure with almost no opening of the pores until 1 bar.

Magnetic Properties. All magnetic studies have been performed on polycrystalline samples of ground single crystals. The dehydrated compound **2** was generated directly in the susceptometer by heating the sample to 373 K for 5 min. The magnetic behaviors for **1rac**, **1*R***, and **1*S*** are the same as could be anticipated from the structural features. In the following, we use the data obtained for **1*S*** to illustrate the magnetic features of these compounds; the data for **1rac** and **1*R*** are provided as Supporting Information for comparison. The magnetic behavior obtained for compound **1*S*** (Figure 5) revealed that it behaves as a magnet below a temperature of $T_{C1} = 85$ K. The temperature dependence of the field cooled magnetization (FCM) recorded in a field of 100 Oe shows a strong and abrupt rise of the magnetization value below 90 K featuring long-range magnetic ordering. This is confirmed by the remnant magnetization (REM) that vanishes only above 85 K. The variation of $\chi_M T$ versus T (χ_M stands for the molar magnetic susceptibility) given in Figure SI4 (Supporting Information) shows a $\chi_M T$ value of 14.06 $cm^3 \cdot K \cdot mol^{-1}$ at 300 K in good agreement with the expected value of 13.9 $cm^3 K mol^{-1}$ for two low spin Mo^{III} ($S = {}^1/_2$) and three Mn^{II} ($S = {}^5/_2$) ions without interactions. Below this temperature the value of $\chi_M T$ increases slightly, but continuously, as T is lowered to 90 K where a steep increase is observed reaching a maximum at 75 K. The temperature dependence of the AC magnetic susceptibility for compound **1*S*** was measured with an oscillating field of 3 Oe for a frequency of 100 Hz in the absence of a static field. The values for χ''_M become different from zero for temperatures below 85 K, confirming the occurrence of a magnetic ordering for $T_{C1} = 85$ K (Figure SI4). The field dependence of the magnetization recorded at 2 K (Figure 6) indicates that magnetization reaches saturation with Ms = 12.64 μ_B already for low fields. This value is consistent with antiferromagnetic Mo−Mn interactions in line with previous observations.[15,17,34,50] Compound **1*S*** exhibits also an hysteresis loop with a coercivity of $H_c = 150$ Oe (Figure 7 Insert). Hence, **1*S*** is a soft ferrimagnet ordering at $T_{C1} = 85$ K.

The magnetic behavior of the compound **2*S*** (i.e., after H_2O release) is remarkably changed with respect to compound **1*S***. For **2*S*** magnetic ordering is found at $T_{C2} = 106$ K as shown Figure 7. For this compound the FCM exhibits a steep increase of magnetization for temperatures below 110 K and the REM vanishes only above 106 K. The $\chi_M T$ versus T plot (Figure SI5) shows a $\chi_M T$ value of 14.9 $cm^3 K mol^{-1}$ at 300 K confirming that the spin states for both the Mo and Mn ions are not modified. The χ'_M and χ''_M responses as a function of T from AC measurements (Figure SI5) show that χ''_M deviates from zero for 106 K and temperatures below, confirming the magnetic order for $T_{C2} = 106$ K. The field dependence of the magnetization recorded at 2 K indicates that **2*S*** quickly reaches a saturation magnetization of 12.55 μ_B and reveals a hysteresis loop with $H_C = 90$ Oe (Figure SI6).

Interestingly, modification of the characteristics of the magnet upon solvent release is reversible, and the initial properties are recovered when the material takes back the H_2O molecules. We could check that this sorption process can be repeated several

(40) Yaghi, O. M.; O'Keeffe, M.; Ockwig, N. W.; Chae, H. K.; Eddaoudi, M.; Kim, J. *Nature* **2003**, *423*, 705−714.
(41) Férey, G.; Mellot-Draznieks, C.; Serre, C.; Millange, F. *Acc. Chem. Res.* **2005**, *38*, 217−225.
(42) Serre, C.; Millange, F.; Thouvenot, C.; Noguès, M.; Marsollier, G.; Louër, D.; Férey, G. *J. Am. Chem. Soc.* **2002**, *124*, 13519−13526.
(43) Loiseau, T.; Serre, C.; Huguenard, C.; Fink, G.; Taulelle, F.; Henry, M.; Bataille, T.; Férey, G. *Chem.−Eur. J.* **2004**, *10*, 1373−1382.
(44) Uemura, K.; Matsuda, R.; Kitagawa, S. *J. Solid State Chem.* **2005**, *178*, 2420−2429.
(45) Kitaura, R.; Seki, K.; Akiyama, G.; Kitagawa, S. *Angew. Chem., Int. Ed.* **2003**, *42*, 428−431.
(46) Bourrelly, S.; Llewellyn, P. L.; Serre, C.; Millange, F.; Loiseau, T.; Ferey, G. *J. Am. Chem. Soc.* **2005**, *127*, 13519−13535.
(47) Sudik, A. C.; Millward, A. R.; Ockwig, N. W.; Côté, A. P.; Kim, J.; Yaghi, O. M. *J. Am. Chem. Soc.* **2005**, *127*, 7110−7118.
(48) Llewellyn, P. L.; Bourrelly, S.; Serre, C.; Filinchuk, Y.; Férey, G. *Angew. Chem., Int. Ed.* **2006**, *45*, 7751−7754.
(49) Chen, B.; Liang, C.; Yang, J.; Contreras, D. S.; Clancy, Y. L.; Lobkovsky, E. B.; Yaghi, O. M.; Dai, S. *Angew. Chem., Int. Ed.* **2006**, *45*, 1390−1393.
(50) Le Goff, X. F.; Willemin, S.; Coulon, C.; Larionova, J.; Donnadieu, B.; Clérac, R. *Inorg. Chem.* **2004**, *43*, 4784−4786.

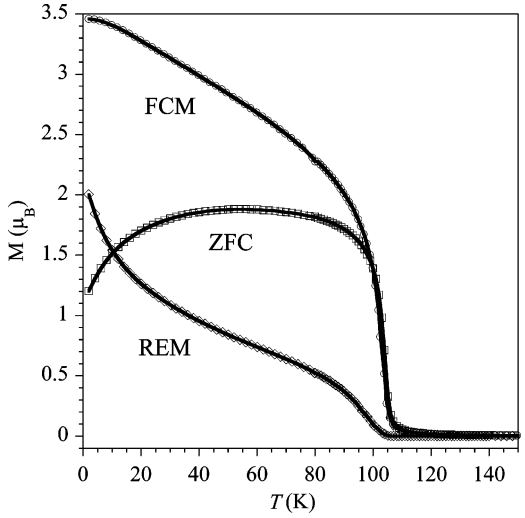

Figure 7. Field cooled magnetization (○, $H = 100$ Oe), zero field cooled (□), and remnant magnetization (◇) as a function of temperature for the dehydrated compound **2*S***.

times without any noticeable alteration of the magnetic features for phases **1*S*** and **2*S***. Hence, these compounds (*S*-, *R*-, and *rac*- isomers) are magnets with an ordering temperature that can be switched back and forth from $T_{C1} = 85$ K to $T_{C2} = 106$ K depending upon the sorption state. The efficiency of the sorption process and hence the switching feature are directly related to the open framework exhibited by the compound. It is worth mentioning that this switching between T_{C1} and T_{C2} is very sharp; no intermediate ordering temperature or gradual shift was observed even when the sample was partially dehydrated. In the latter case, only the signatures of **1*S*** and **2*S***, i.e., T_{C1} and T_{C2}, were found in the magnetic data.

The rather high T_C's exhibited by these magnets rely on the use of a spin carrier (Mo) of the second row transition metal characterized by a magnetic orbital with more spatial extension than the 3d metal ions.[51] However, the origin of the significant difference of T_C ($T_{C2} = T_{C1} + 21$ K) for the hydrated and dehydrated compounds is found in the coordination sphere of the Mn ions. In a previous study dealing with [Mn/{Mo(CN)$_7$}] magnets, we have shown that T_C is also related to the coordination geometry of the Mn ions and does substantially increase when the number of ancillary ligands (for instance H_2O) in the coordination sphere of the Mn is reduced.[15] This is understood by the decrease of the Mn←NC bond lengths observed when going from an octahedral to a tetrahedral geometry which lead to a better overlap of the metal and ligand orbitals and consequently to stronger exchange interactions. For compounds **1*S***, **1*R***, and **1*rac***, one Mn site has a tetrahedral geometry (MnA) and the second (MnB) exhibits a six-coordinated surrounding with a H_2O ligand. After dehydration, all of the H_2O contained in **1*S***, **1*R***, **1*rac*** have been released including those linked to the MnB sites. Consequently, compounds **2*S***, **2*R***, and **2*rac*** still possess the tetrahedral MnA sites, but the MnB are now five coordinated. As mentioned above, this reduced coordination number leads to shorted Mn−NC bonds for MnB and therefore to stronger {Mn−Mo} exchange interactions, which in turn shift T_C to higher temperatures (i.e., $T_{C2} = 106$ K). When the framework takes back the H_2O, the MnB sites recover their six ligand surroundings and the magnet exhibits its initial features with $T_{C1} = 85$ K.

(51) Visinescu, D.; Desplanches, C.; Imaz, I.; Bahers, V.; Pradhan, R.; Villamena, F.; Guionneau, P.; Sutter, J. P. *J. Am. Chem. Soc.* **2006**, *128*, 10202−10212.

Concluding Remarks

The reported compounds illustrate the possibility of switching the magnetic feature of a magnet simply by taking advantage of the sorption capability of a porous framework. In the present case, a reversible shift of T_C by 21 K was obtained by means of H_2O release and uptake by the supramolecular framework. Besides, these compounds represent a typical example of multifunctional materials by combining three properties namely magnetism, porosity, and chirality. It is the synergy between the magnetic and zeolitic (i.e., sorption) properties that leads to the switchable T_C. The inter-relation between magnetism and chirality remains to be established for these chiral magnets. Finally, it can be stressed that these magnets possess rather high T_C's which situate them among the very few molecule-based magnets efficient at liquid N_2 temperatures.

Experimental Section

General. All experiments have been conducted in a N_2 atmosphere, the solvents were distilled under N_2, and the reagents were degassed prior to use. $K_4Mo(CN)_7$[52] was prepared as described, *N*,*N*′-dimethylalanine[53] was obtained by an alternative route adapted from a general procedure.[54] Infrared spectra were recorded as KBr pellets in the range 4000−400 cm^{-1} by using an Perkin-Elmer GX 2000 FTIR spectrometer. Magnetic measurements down to 2 K were carried out with a Quantum design MPMS-5S SQUID susceptometer. All magnetic investigations were performed on polycrystalline samples in a gelatin capsule. A diamagnetic correction of -500.10^{-6} cm^{3}mol^{-1} was used to account for the diamagnetic contribution of the compound and the sample holder. NMR was recorded on a Bruker ARX250 spectrometer.

Specific surface areas were measured by N_2 adsorption measurements performed at 77 K using the Brunauer−Emmet−Teller method[55] (BET) on a MICROMERITICS ASAP 2010 analyzer in the relative P/P_0 pressure range from 0.05 to 0.25. The cross-sectional area of a nitrogen molecule was assumed to be equal to 0.162 nm^2. The sample was previously degassed by heating at 100 °C under vacuum (10^{-3} Torr). N_2, CO_2, and CO adsorption experiments were also recorded at 293 K using the same instrument with a 60 s equilibration delay. The equilibrium constants for the gas binding affinity, K_i, and the adsorption capacity, V_i, were calculated by considering two different adsorption processes: a selective adsorption of CO_2 with higher energetic interaction and a nonselective physisorption resulting from low energy adsorption and diffusion of the gas into the solid material.[56−58] The experimental data corresponding to the CO_2 adsorption isotherms were thus analyzed using a model based on two Langmuir-type isotherms (eq 1) while the N_2 and CO ones were fitted with a single Langmuir-type isotherm model (eq 2).

$$V_{CO_2} = \frac{V_1 \cdot K_1 \cdot P}{1 + K_1 \cdot P} + \frac{V_2 \cdot K_2 \cdot P}{1 + K_2 \cdot P} \quad (1)$$

(52) Young, R. C. *J. Am. Chem. Soc.* **1932**, *54*, 1402−1405.
(53) Bowman, R. E.; Stroud, H. H. *J. Chem. Soc.* **1950**, 1342−1345.
(54) Borch, R. F.; Hassid, A. I. *J. Org. Chem.* **1972**, *37*, 1673−1674.
(55) Brunauer, S.; Emmet, P. H.; Teller, E. *J. Am. Chem. Soc.* **1938**, *60*, 309−319.
(56) Dubois, G.; Tripier, R.; Brandès, S.; Denat, F.; Guilard, R. *J. Mater. Chem.* **2002**, *12*, 2255−2261.
(57) Barbe, J.-M.; Canard, G.; Brandès, S.; Jerome, F.; Dubois, G.; Guilard, R. *Dalton Trans.* **2004**, 1208−1214.
(58) Barbe, J. M.; Canard, G.; Brandès, S.; Guilard, R. *Chem.—Eur. J.* **2007**, *13*, 2118−2129.

$$V_i = \frac{V_1 \cdot K_1 \cdot P}{1 + K_1 \cdot P} \qquad \text{with } i = N_2 \text{ or CO} \qquad (2)$$

$Me_2NCH(Me)COOH$. (Performed in air) To a stirred solution of D-, L-, or DL-alanine (5 g, 56.1 mmol) in CH_3CN (150 mL) and 37% aqueous formaldehyde (20 mL, 0.25 mol) cooled in an ice bath was added (by small portions) sodium cyanoborohydride (5.45 g, 86.7 mmol). The reaction is exothermic and leads to the formation of a white "cottonlike" precipitate. The reaction mixture was stirred for 15 min, and then glacial acetic acid was added dropwise until the solution tested neutral on wet pH paper. Stirring was continued for an additional 45 min, glacial acetic acid being added occasionally to maintain the pH near neutrality. The solvent was evaporated at reduced pressure, and 2 N KOH (200 mL) was added to the residue. The resulting mixture was extracted with Et_2O (3 × 100 mL). The combined ether extracts were washed with a 0.5 N KOH solution (total 200 mL). The basics solutions are then combined together and concentrated under reduced pressure (to ca. 200 mL) and then acidified to pH = 2 with concentrated HCl. The white crystalline precipitate of salts formed upon standing overnight is filtered off, and the filtrate is concentrated another time until the appearance of salts. This process is repeated 4 times. The ultimate filtrate is then completely evaporated to obtain a very hygroscopic white powder of $Me_2NCH(Me)COOH$ in quantitative yield. This compound was used for the next step without further purification. ^{1}H NMR (200 MHz, D_2O) : δ = 1.56 (d, 3H, J = 7.3 Hz, Me), 2.83 and 2.90 (2s, 6H, NMe_2), 3.89 (q, 1H, J = 7.3 Hz, CH).

$Me_2NCH(Me)CH_2OH$·HCl (L·HCl). The reduction of $Me_2NCH(Me)COOH$ was conducted as described earlier.[59] After purification *N*,*N*′-dimethylalaninol was dissolved in H_2O and concentrated HCl was added until pH = 2 was reached. The solvent was removed under reduced pressure, and **L**·HCl was obtained as a very hygroscopic white solid. ^{1}H NMR (250 MHz in D_2O): for **L**·HCl: δ = 1.27 (d, 3H, J = 6.9 Hz, CH*Me*), 2.89 and 2.78 (2s, 6H, NMe), 3.52 (m, 1H, C*H*Me), 3.68 and 3.87 (2dd, 2H, ^2J = 12.8 Hz, ^3J = 4.1 and 8.2 Hz, CH_2); for **L**: δ = 0.96 (d, 3H J = 6.7 Hz, CH*Me*), 2.18 (s, 6H, NMe), 2.61 (m, 1H, C*H*Me), 3.43 and 3.62 (2dd, 2H, ^2J = 11.4 Hz, ^3J = 5.6 and 6.4 Hz, CH_2). L-(*S*)-**L**·HCl: $[\alpha]_D^{20} = +20 \pm 5$ ($c = 10.2.10^{-3}$ g/mL in H_2O for λ_{578}); d-(*R*)-**L**·HCl: $[\alpha]_D^{20} = -23 \pm 5$ ($c = 10.2.10^{-3}$ g/mL in H_2O for λ_{578}). In order to check the stability of these chiral molecules in solution, the $[\alpha]_D^{20}$ of these solutions were measured regularly over a period of 50 days; no modification of the initial values was found.

[{Mn(HL)(H_2O)}$_2$Mn{Mo(CN)$_7$}$_2$]·2H_2O, 1. (As a microcrystalline powder) A solution of $MnCl_2$·4H_2O (566 mg, 2.86 mmol) and **L**·HCl (303 mg, 2.17 mmol) in H_2O (20 mL) was added slowly with a canula to a stirred solution of $[K_4Mo(CN)_7]$·2H_2O (670 mg, 1.43 mmol) in H_2O (20 mL) leading to the formation of a green solid. The mixture was further stirred for 15 min and filtered under nitrogen. The solid was washed with H_2O (4 × 20 mL), followed by EtOH (20 mL) and Et_2O (15 mL), and subsequently dried by flushing with a N_2 stream yielding **1** (606 mg, Y = 85%) as a microcrystalline dark-green powder. Analyses calculated for $C_{24}H_{28}N_{16}O_2Mo_2Mn_3$ + 4H_2O: C, 28.79%; H, 3.62%; N, 22.38%. Found: C, 28.0%; H, 2.4%; N, 22.6%. (Note: the deviation found for the H analysis is due to the small H content that is below the limit of detection of the apparatus used.)

(As single crystals) In a Schlenck tube, an acidic H_2O solution (12 mL with 0.3 mmol HCl) of $[K_4Mo(CN)_7]$·2H_2O (94 mg, 0.2 mmol) and **L**·HCl (30 mg, 0.21 mmol) was allowed to slowly diffuse into a H_2O (5 mL) solution of $MnCl_2$·4H_2O (60 mg, 0.30 mmol). After few days needle-shaped dark-green crystals (*ca.* 8 mg) are formed together with a crystalline powder. Analyses calculated for $C_{24}H_{28}N_{16}O_2Mo_2Mn_3$ + 4H_2O: C, 28.79%; H, 3.62%; N, 22.38%. Found for **1*S***: C, 27.9%; H, 2.9%; N, 21.9%. For **1*rac***: C, 27.7%; H, 3.0%; N, 21.9%. IR (cm^{-1}): 3581 (m), 3440 (m broad), 2918 (w), 2851 (w), 2092 (s with shoulders at 2145, 2126, 2105), 1634 (m), 1466 (m), 1434 (w), 1412 (w), 1393 (w), 1064 (w), 1032 (m).

Solutions and Refinement of the X-ray Structures: Single crystals were selected on a polarized microscope and mounted on a Bruker-Nonius κ-CCD diffractometer, Mo Kα radiation (0.710 73 Å). Data collections were performed at 293 K using mixed ϕ and ω scans. The structural determination was carried out by direct methods, and the refinement of atomic parameters based on full-matrix least-squares on F^2 was performed using the SHELX-97[60] programs within the WINGX package.[61]

Acknowledgment. This work was supported by the European Union through a grant to J.M. The authors wish to express their thanks to Dr. J. C. Daran (LCC Toulouse) for fruitful discussions on the crystallographic investigations of the chiral magnet.

Supporting Information Available: Crystallographic details for **1*S*** and **1*rac*** in cif format, ORTEP plot for **1*S*** and **1*rac***, XRPD of a powder sample of **1 *rac***, SHAPE analysis data, IR spectra of **1*S*** and **2*S***, $\chi_M T$, χ' and χ'' versus T plots for **1*S*** and **2*S***, M versus H for **2*S***, plots of the magnetic behaviors for **1*rac***, **1*R***, **2*rac***, and **2*R***. This material is available free of charge via the Internet at http://pubs.acs.org.

JA073612T

(59) Hayashi, T.; Konishi, M.; Fukushima, M.; Kanehira, K.; Hioki, T.; Kumada, M. *J. Org. Chem.* **1983**, *48*, 2195−2202.

(60) Sheldrick, G. M., Ed. *Programs for Crystal Structure Analysis*, release 97-2; University of Göttingen: Germany, 1998.

(61) Farrugia, L. J. *J. Appl. Crystallogr.* **1999**, *32*, 837.